Transactions of the TSME (2019) Vol. 7, No. 1, 11-22
Journal of Research and Applications in Mechanical Engineering

ISSN 2229-2152 print
DOI: 10.14456/jrame.2019.2

Research Article

NUMERICAL STUDY OF RESISTANCE AND FORM FACTOR OF HIGH-SPEED CATAMARANS

S. Srinakaew[1,*]
D. J. Taunton[2]
D. A. Hudson[2]
[1] Department of Marine Engineering, Royal Thai Naval Academy, 204 Sukhumvit Road, Paknam, Samut Prakan, Thailand, 10270
[2] Fluid-Structure Interaction Group, University of Southampton, Burgess Road, Southampton, SO16 7QF, UK

Received 25 February 2019
Revised 2 May 2019
Accepted 7 May 2019

ABSTRACT:
Since the prediction of resistance of the full-scale ship mainly relies on extrapolation of form factor of the model, it is important to determine the form factor precisely. Nowadays, the computer performance has been developed, commercial CFD code with Reynolds-averaged Navier-Stokes Equations (RANS), which is widely accepted and used by many researchers is capable of determining resistance components. This paper presents the development and procedures for the prediction resistance components and form factor of displacement catamarans by using commercial CFD code, STAR CCM+, with SST k-ω turbulence model. The Wigley catamarans with three hull configurations including S/L = 0.2, 0.3 and 0.4 are investigated at Froude number between 0.2 and 0.8. Resistance components, which are total (C_T), skin friction (C_F), viscous (C_V), residual (C_R) and wave (C_W) resistance, form factor (1+k), form resistance interference factor (β), wave resistance interference factor (τ) and wave elevation along the hull are estimated and validated against experiment retrieved from Insel (1992). The results show that CFD code with RANS equations is capable of estimating resistance components and demonstrates that form factor increases with speed (Fn).

Keywords: *Computational Fluid Dynamics (CFD), Form factor, Wigley Hull*

1. INTRODUCTION

There are various approaches used to estimate resistance and form factor for the displacement vessel. These approaches include the most reliable method – experiment, numerical approaches e.g. thin ship theory and computational fluid dynamics (CFD), and empirical formula. The examples of the use of experimental approach for determining resistance components and form factor of displacement vessels have been found in many works. Insel and Molland conducted the experimental series of displacement ships at University of Southampton. The experimental results for NPL and Wigley hull series were compared with the thin ship theory [1]. A further set of experiment for the high-speed catamarans in the finite water depth is found in [2] with the range of Froude numbers between 0.25 and 1.2.

The use of CFD technique to estimate resistance components using different codes is found in [3], [4] and [5]. The examples of those CFD codes with RANS equations are CFX™, Fluent and STAR CCM+. The CFD code with Slender Body Theory used in [4] to estimate the resistance for catamarans is SHIPFLOW. The separation to length ratio is recommended not to exceed 0.6 as the interference effects between demihulls are demolished. The use of stead state simulation with Volume of Fluid Method can be found in [5]. These are the evidence that the CFD code can be used to calculate resistance components for catamarans.

* Corresponding author: S. Srinakaew
E-mail address: s.srinakaew@gmail.com

The CFD codes are also used to investigated free surface flow characteristics as seen in [6], [7] and [8]. As the numerical investigation procedures, the results were compared against another numerical models such as Boundary Element Method (BEM) and experiments and the results showed an acceptable agreement. Apart from that, to reduce the numerical wall time, the model was fixed with sinkage and trim with the experiment as found in [9] and [10]. However, there were just some certain Froude numbers were focused and results were presented both resistance and wave cuts.

Since resistance prediction for a full-scale ship mainly relies on the extrapolation of a form factor, it is important to calculate resistance of models precisely. Froude [11] and Hughes [12] introduced approaches was form effect is taken into account in the extrapolation procedure. Thereafter, International Towing Tank Conference (ITTC) adopted this approach as the recommendation. Form factor (1+k) is the dependence of Reynolds number (Re) and suggested by ITTC Resistance Committee that Reynolds number plays an important role in varying (increase) form factor. CFD codes were also used to investigate the scale effects on form factor which are found in [13, 14] and [15]. ITTC 2002 [16] also suggested that correlation line might deter the estimation of form factor.

From the literature, it can be seen that CFD code is capable of being used as the numerical tool to investigate resistance and form factor of high-speed catamarans. This study proposes the numerical procedures in estimating resistance components and form factor of Wigley III catamarans and their dependence on speed (Fn).

2. CATAMARAN RESISTANCE

The broken down of resistance components dependent on Froude number and Reynolds number and recommended by ITTC is shown in equation (1).

$$C_T(Fn, Re) = C_V(Re) + C_W(Fn) = (1+k)C_F(Re) + C_W(Fn) \quad (1)$$

Resistance for the catamarans are summarized by [2], which the interference effects between demihulls are added to consideration. Two types of interference that are considered including viscous resistance and wave resistance interference. Hence, equation (1) becomes (2) and (3) for catamaran.

$$C_{Tcat} = (1+k_{cat})C_{Fcat} + C_{Wcat} \quad (2)$$

$$C_{Tcat} = (1+\beta k)C_F + \tau C_W \quad (3)$$

Where, β is viscous resistance interference factor and τ is wave resistance interference factor.

3. NUMERICAL SETTING AND GRID GENERATION

3.1 Hull Geometry

Wigley III is used in the simulation to minimize the problems due to the complex flow characteristics and separations in the region of the transoms. Hull particulars are shown in Table 1 and Fig. 1. This hull is selected over other hulls in the Wigley series because it has the highest hull slenderness, which is more representative of high-speed displacement catamarans. The Wigley hull was created from the right-handed side coordinate system mathematical formulation defined by O(ξ,η,ζ), as shown in equation (4).

$$\eta = B/2\,[1-(\zeta/T)^2\,][1-(2\xi/L)^2\,][1+a\_2\,(2\xi/L)^2\,] \quad (4)$$

Where, O is original amidships in the water plane
ξ is longitudinal axis, positive forwards
η is lateral axis, positive to port side
ζ is vertical axis, positive downward
$a_2 = 0.2$ for all models

Table 1: Wigley III hull particulars

Model	**Wigley III**
L, *m*	1.80
L/B	10.00
B/T	1.60
$L/\nabla^{1/3}$	7.116
C_B	0.444
C_P	0.667
C_M	0.667
WS, m^2	0.482

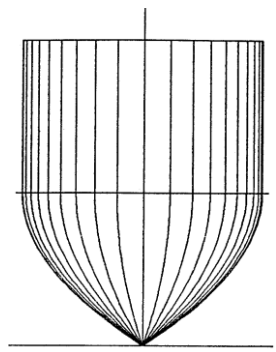

Fig. 1. Wigley III [2]

3.2 Numerical Domain and Grid Generation

The distance between the hull geometry and boundaries need to be far enough to allow undisturbed wave system around the hull to propagate fully and to avoid reflections. Hence, the domain inlet boundary is 3L from bow and outlet is located 9L from stern. To reduce the numerical wall time and number of cells, a symmetry plane is also used [17]. The numerical domain dimensions are presented in Table 2 and Fig. 2.

Table 2: Numerical domain

Hull length, *m*	L	1.80
Tank width, *m*	W	1.85
Tank depth, *m*	D	1.80
Air, *m*	D_a	1.00
Inlet from bow	L_i	3L
Outlet from stern	L_o	9L

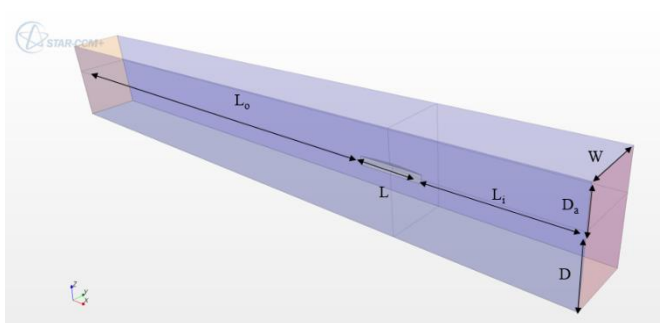

Fig. 2. Numerical domain

From the literatures it is found that total number of cells association with grid density and coasenness can affect the accuracy of the results. Some papers suggested that number of cells is about million cells. the total number of cells is dependent on hull geometry, numerical domain size and flow chacteristics i.e. flow separation, wave elevation and transition flows. According to the auther's previous published work [17], the total cells are approximately 5 – 6 M.

Grid refinement blocks are used to control the number of cells, transition area and coarsenness of the grid. Refinement block shape and size are created in consideration of the wave system and flowfield. The refinement blocks are placed around the hull, bow and stern, separation area between demihulls, free surface, wake behind stern and wave system propagation from the hull. The representation of grid creation can be seen in Figs. 3 a) and b).

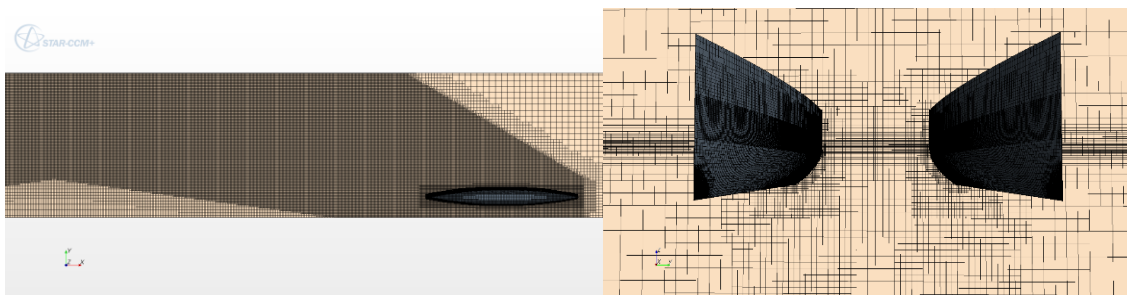

a) b)

Fig. 3. Grid generation for farfiled area and free surface a), and around demihulls the hull and free surface b)

SST k – ω turbulence model with all wall function is used in this investigation since the the litteratures pointed out that this model gives an accepted and accurate results. This turbulence model is used because it blends wall function of low and high wall y^+, which gives a similar results with low and high wall function when the grids fall into the buffer region, $1 < y^+ < 30$.

3.3 Methodology

In this investigation the hull geometry is run with a fixed trim and sinkage replicated the experiment conducted by Insel [1]. Hence, the simulation in this study is steady state in which there are no hull motions.

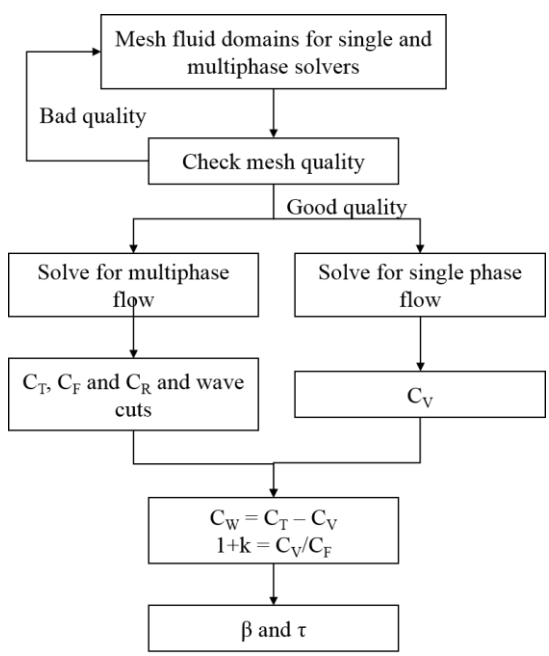

Fig. 4. Computational methodology flow chart

Figure 4 presents the precedure for the computational methodology, which starts by constructing the mesh for solvers. All mesh qualities are checked if they are not good enough. The multiphase flow solver gives the total, skin friction and residual resistance while the single phase solver gives the viscous rsistance. The wave resistance is calculated by subtracting C_V from C_T. Afterwards, form resistance interference and wave resistance interfence factors are estimated.

4. RESULTS

Resistance components are retrieved from the CFD code including C_T, C_F, and C_V. Total resistance is measured from the sum of pressure and shear forces available in the CFD package. C_V can be obtained by applying a double-model method, which assumes that there is no free surface flow. Three hull configurations are presented including S/L = 0.2, 0.3 and 0.4 respectively.

4.1 Total, Skin Friction and Viscos Resistance Components

Total, skin friction and viscous resistance coefficients are presented in the same graph in order to demonstrate the magnitudes of resistance components used in determining form factor, which can be seen in Fig. 5. The CFD results are validated against [2]. Total and viscous resistance components are validated against the experiment whilst skin friction is compared with the ITTC correlation line. The reference viscous resistance coefficients from the experiment is calculated using the average form factor from Insel's experiment multiplied by the ITTC skin friction coefficients.

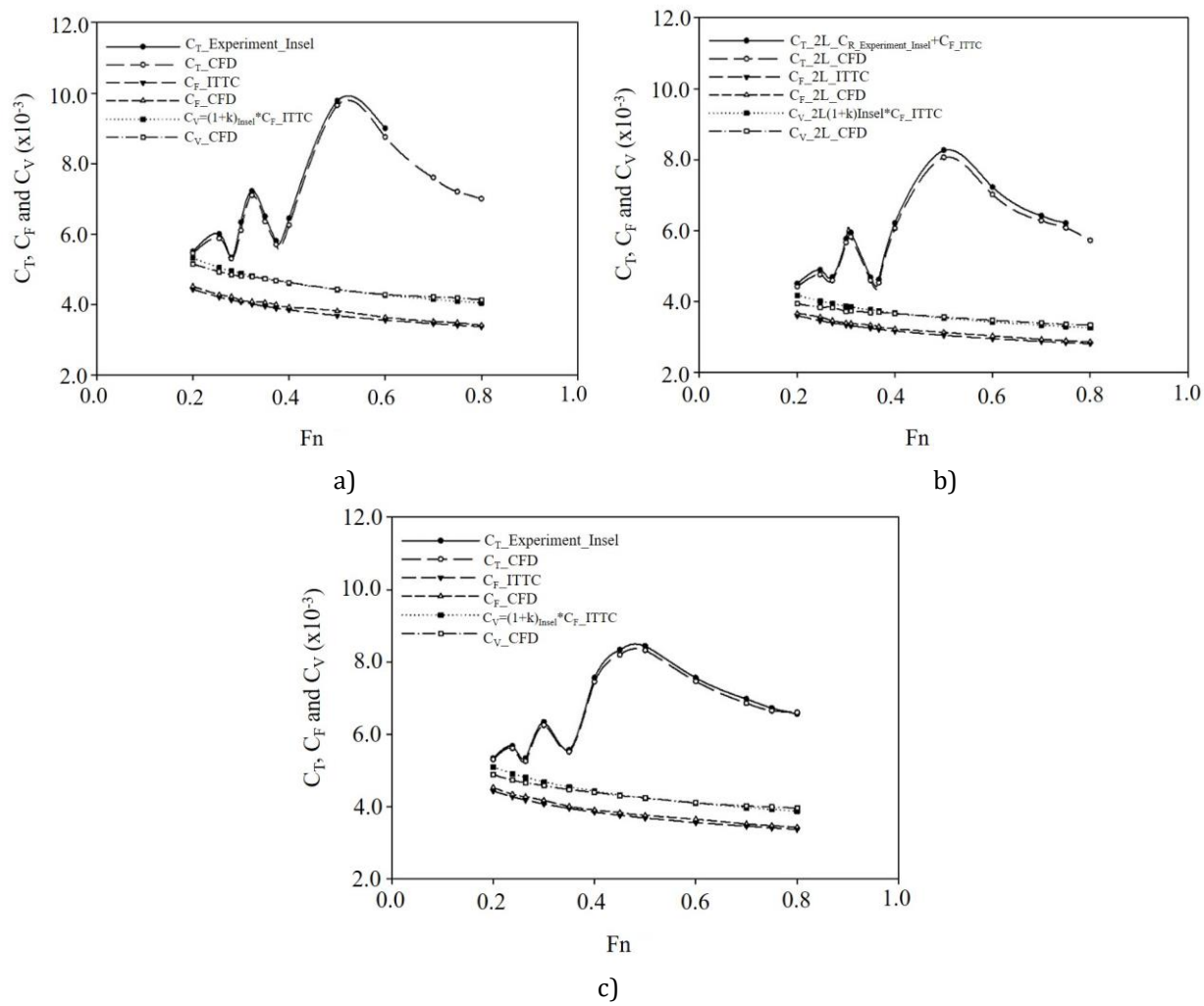

Fig. 5. Resistance components for a) S/L 0.2, b) S/L 0.3 and c) S/L 0.4

4.2 Residual and Wave Resistance Components

Figure 6 shows the validation of residual and wave resistance components against experimental data. Residual resistance used as validated data is from Insel's experiments and determined by subtracting the ITTC skin friction resistance coefficient from experimental total resistance while CFD residual resistance is determined from analysis of the pressure force. The reference wave resistance component is calculated by subtracting viscous resistance component from total resistance component. CFD wave resistance is determined using the same method with the validation data which the viscous resistance components is calculated by applying the double-model approach.

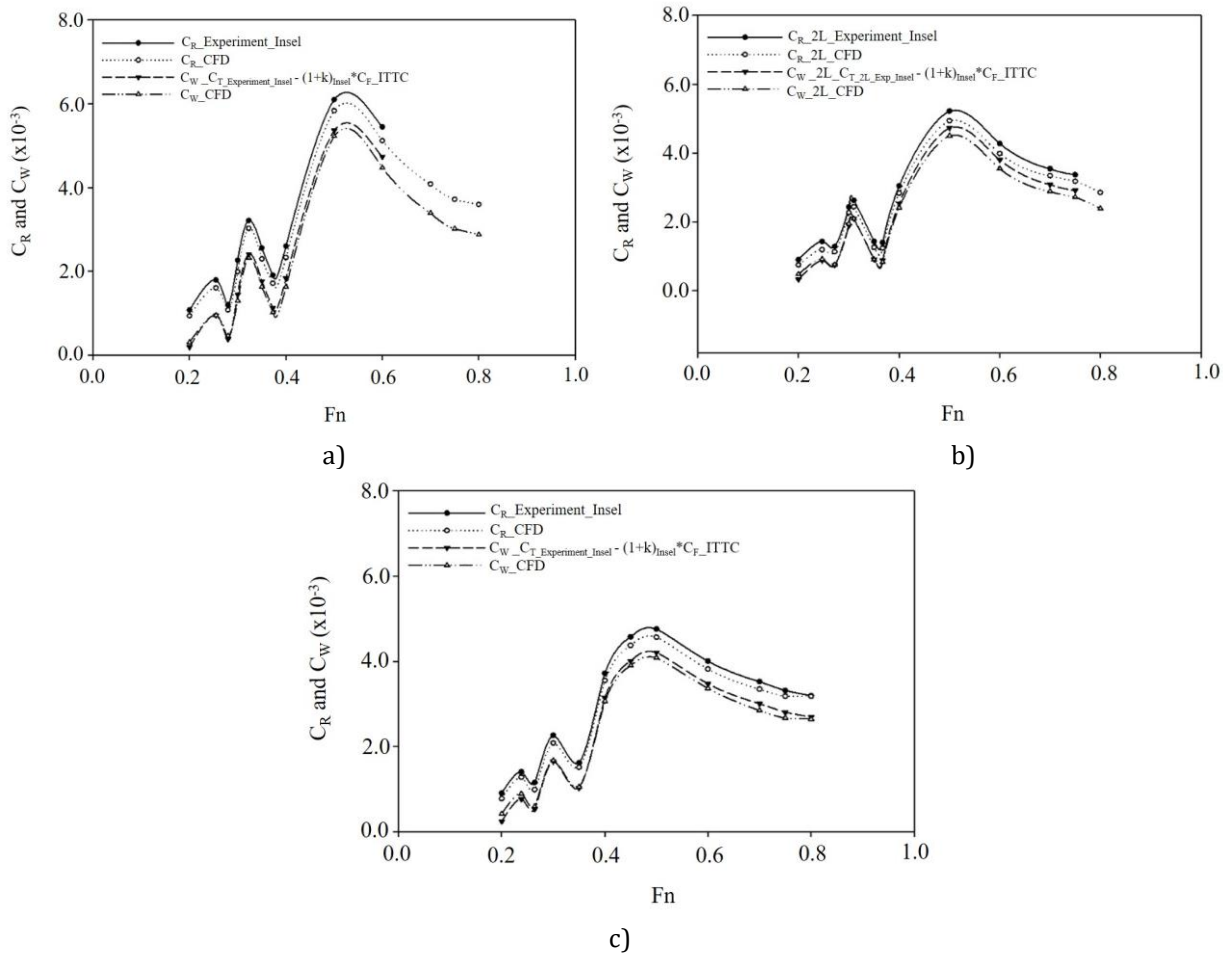

Fig. 6. Resistance components for a) S/L 0.2, b) S/L 0.3 and c) S/L 0.4

4.3 Form Factors

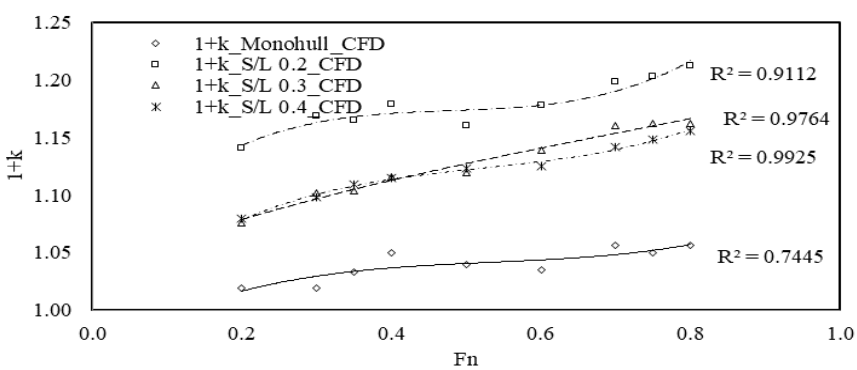

Fig. 7. Form factor for different hull separations

4.4 Form Resistance and Wave Resistance Interference Factors

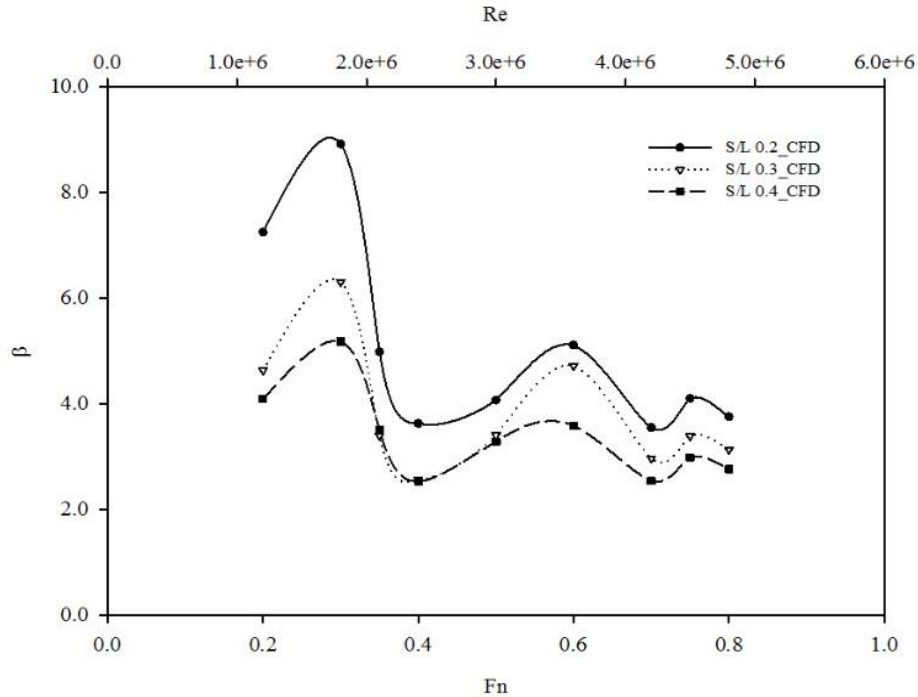

Fig. 8. Form resistance interference factor

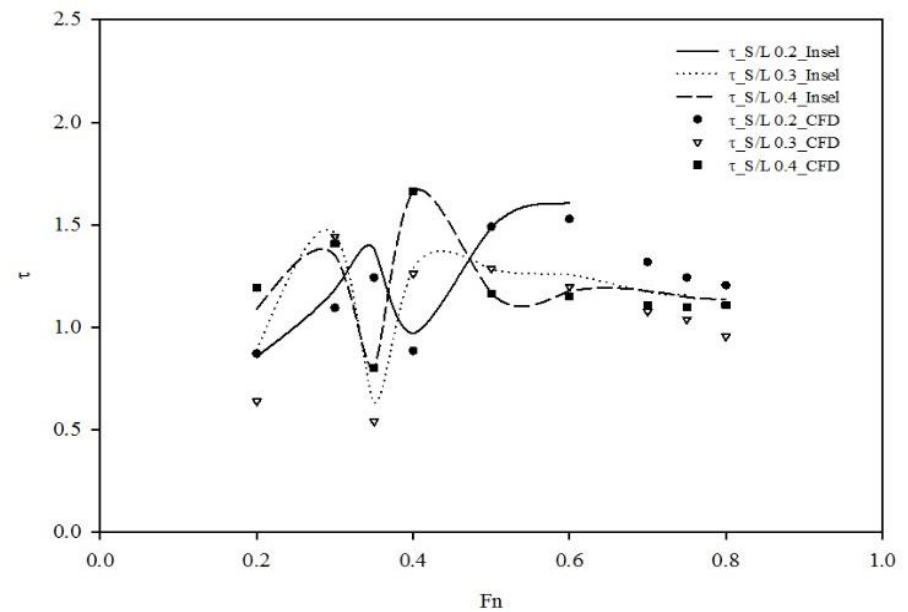

Fig. 9. Wave resistance interference factor

Form resistance interference factor is presented in Fig. 8. The form resistance interference factor is the proportion between the form resistance of a monohull and a catamaran. There are no validations presented in this section due to the fact that Insel's experimental form resistance is constant over the entire range of Froude numbers for given hull separation. Fig. 9 presents the wave resistance interference factor. This resistance interference factor is the proportion between wave resistance of a monohull and a catamaran. The validation is also made against Insel's experimental data.

4.5 Wave Elevation along the Hull

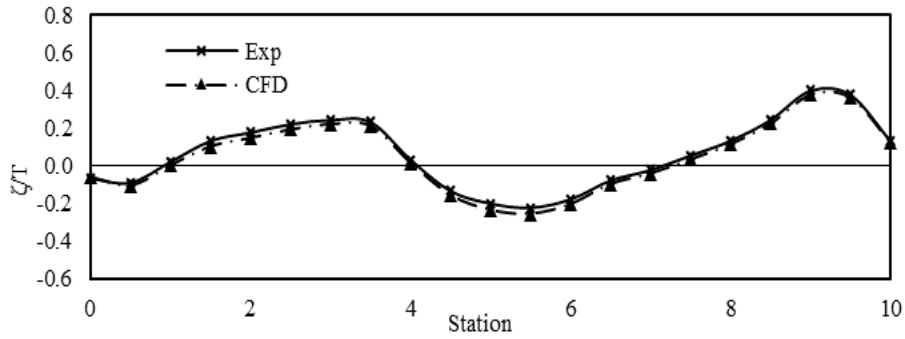

a)

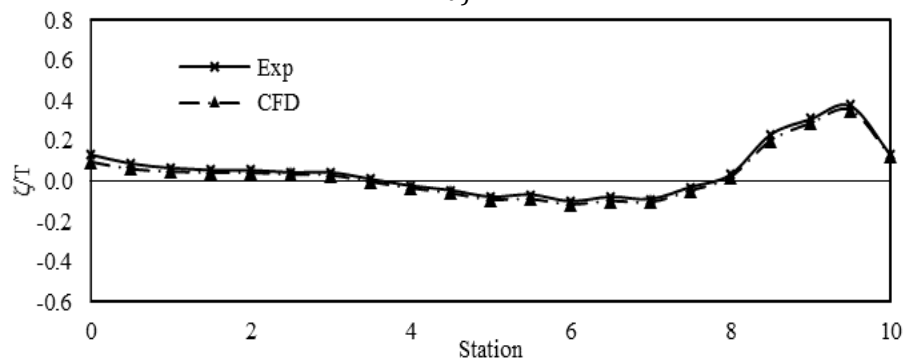

b)

Fig. 10. Wave elevation along the hull for S/L = 0.2 at Fn = 0.35 for a) inboard and b) outboard

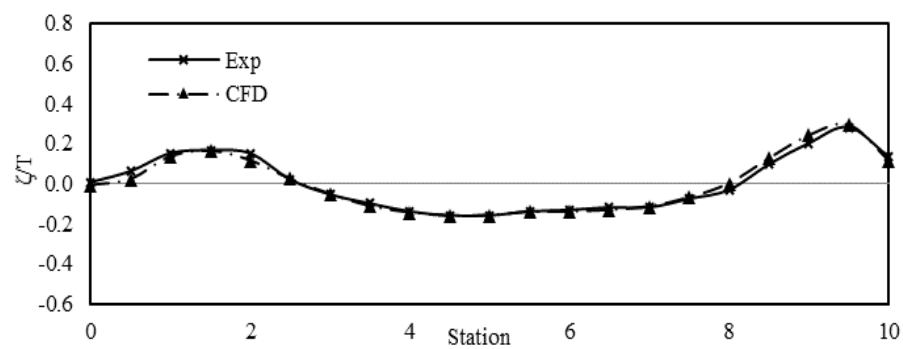

a)

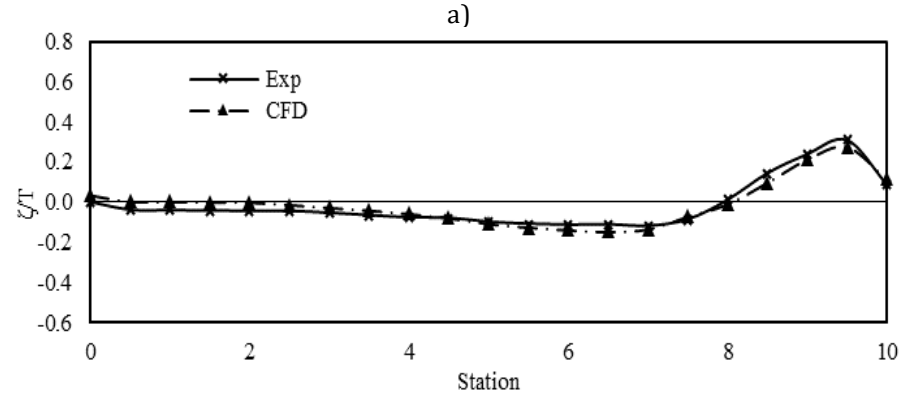

b)

Fig. 11. Wave elevation along the hull for S/L = 0.3 at Fn = 0.35 for a) inboard and b) outboard

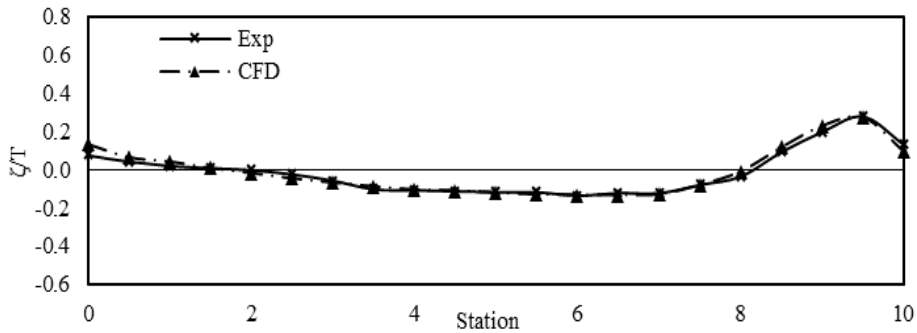

a)

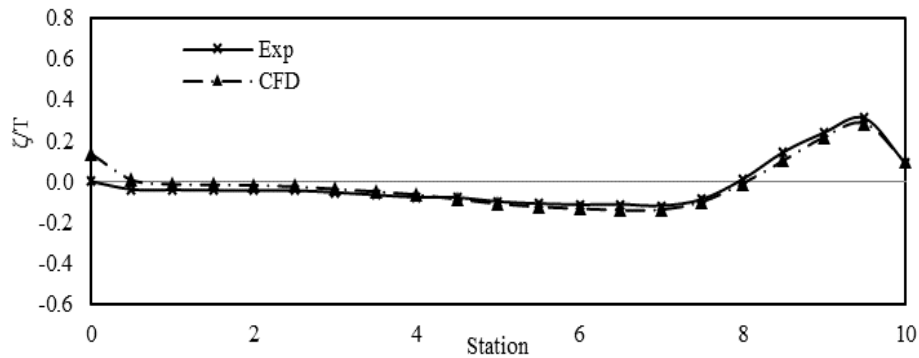

b)

Fig. 12. Wave elevation along the hull for S/L= 0.4 at Fn = 0.35 for a) inboard and b) outboard

5. DISCUSSION AND CONCLUSION

5.1 Discussion

Resistance components including C_T, C_F, C_V, C_R and C_W show a good agreement with the experiment over the range of Froude numbers for all hull configurations as shown in section 4.1 and 4.2, see Figs. 5 and 6. Form factor (1+k) for catamarans are presented in section 4.3 and Fig. 7. Form resistance and wave resistance interference factors are shown in Figs. 8 and 9 respectively. There are three separations to length ratios (S/L) including 0.2, 0.3 and 0.4. These S/Ls are used because the literature shows that at very large separation the interference effect has less influence on resistance. The ranges of Froude numbers in each model are different depending on the availability of experimental data [1].

- *S/L 0.2*

The S/L = 0.2 shows a good agreement with experiment for C_T and C_F while C_V is slightly smaller than experiment for the range of Froude numbers, Fn > 0.4, see Fig. 5 a). The comparison for total resistance can be made only for Fn < 0.8 due to the availability of experimental data. This limitation was caused by water spray for the narrow hull separation. Viscous resistance is under predicted for Fn < 0.3, and then agree very well with experiment. Fig. 6 a) shows the residuary and wave resistance which show a satisfactory agreement with the experiment. The under prediction of residual resistance is that skin friction obtained from CFD code is slightly lower than ITTC correlation line. Wave resistance for Fn < 0.3 is over prediction compared with the experiment.

The experimental data shows that the average form factor is about 1.20 whilst the average form factor calculated using CFD code is about 1.173. Form factor obtained from CFD code shows the increment trend which increases from 1.140 to 1.212, see Fig. 7. The increment of (1+k) shows a small fluctuation, which is higher on either end of Froude number range, Fn < 0.4 and Fn > 0.6. Viscous resistance interference factor (β) is estimated and presented in Fig. 8. CFD results give the highest value at a Froude number of 0.3 of about 8.70. Wave resistance interference factor (τ), shown in Fig. 9, presents a good agreement with experiment. For Fn > 0.5, wave resistance interference factor to decrease linearly. The wave cuts are also measured on both sides of the demihull, the results can be seen in

Fig. 10. Wave elevation along the hull shows a good agreement with experiment; however, it is slightly lower for the inboard cut.

- *S/L 0.3*

Resistance results for S/L = 0.3 are presented in Figs. 5 b) and 6 b). Resistance components calculated using CFD show a good agreement with experiments. CFD C_T shows a good agreement with experiment for lower Froude numbers, Fn < 0.5. For Fn > 0.5, the differences between experiment and CFD results seem to be slightly higher than lower Froude numbers. The prediction of viscous resistance coefficient shows a good agreement with experiment. However, the error is very high at lower Froude numbers, Fn < 0.3.

The CFD average form factor is 1.119 compared with 1.16 for experimental form factor. Form factor seems to increase with speed (Fn) as shown in Fig. 7. The curve fit of form factor for S/L = 0.3 shows slightly different from other hull configurations, which is quite linear. Viscous resistance interference factor (β), presented in Fig. 8, shows the same trend with the narrowest hull separation. Fig. 9 shows wave resistance interference factor (τ) which is validated against the experiment and shows a good agreement with experiment. Unlike the S/L = 0.2, the inversion of fluctuation of wave resistance interference factor is occured. Wave elevations along the hull are shown in Fig. 11 and show a good agreement with experiment.

- *S/L 0.4*

Resistance components for S/L = 0.4 are presented in Figs. 5 c) and 6 c). CFD resistance components show a good agreement with experiment but yield slightly lower values than the experiment. Total resistance coefficient agrees very well with experiment for lower Froude numbers, Fn < 0.5. The differences of total resistance between CFD and experiment are slightly higher for Fn > 0.5. The CFD C_F shows a good agreement with ITTC correlation line with small error. The CFD C_V shows a good agreement with experiment; however, the differences are high for the low Froude numbers, Fn < 0.3, which is similar with other hull configurations. The CFD C_R and C_W show a good agreement with experiment which are particularly low.

Form factor calculated using CFD code, shown in Fig. 7 is about 1.119 while experiment data is about 1.15. Characteristic of form factor is similar with other hull configuration, which increases with Froude number. Viscous resistance interference factor (β), presented in Fig. 8, shows a similar trend with other hull configurations. The differences between S/L 0.3 and 0.4 are resulted from the differences of form factor of these two hulls. Wave resistance interference factor (τ) also shows a good agreement with experiment with a fluctuation at 0.3 < Fn < 0.5, see Fig. 9. For Fn > 0.5, wave resistance interference factor seems to be steady with small gradient. Wave cuts along the hull on both sides, presented in Fig. 12, are validated against experiment and show a good agreement for Fn = 0.35.

5.2 Conclusion

Resistance components of Wigley III catamarans are evaluated and validated against experimental data. Three separations to length ratio are evaluated, 0.2, 0.3 and 0.4. Models are fixed with sinkage and trim determined from Insel's experiments. Total, skin friction and residual resistance are directly measured from CFD code. The double-model approach, without free surface, is used to determine viscous resistance coefficient, C_V. The wave cut along the hull is also made at Froude number 0.35 due to the availability of experimental data from Insel.

To this point, it can be seen that the CFD results show a good agreement with experiments for all separation ratios. All resistance components decrease as S/L increases. Viscous resistance interference factor (β) shows that the highest value is at the Fn = 0.3 for all hull configurations and seems to decrease with speed (Fn). Wave resistance interference factor (τ) also gives a good agreement with experiments. Form factors (1+k) from Insel's experiments decreases when separation increases, which are 1.20, 1.16 and 1.15 for S/L 0.2, 0.3 and 0.4 respectively. The average form factors obtained from CFD code, which are 1.173 and 1.119 for S/L 0.2, and 0.3 respectively, show the same trend with experiment as S/L increases. Although the average form factors of S/L 0.3 and 0.4 are nearly the same, form factor at Fn > 0.5 for S/L = 0.3 are much higher than S/L = 0.4.

The results show that numerical study on resistance of the high-speed catamarans using CFD is capable of predicting resistance components and form factor. CFD results also suggest that form factor decreases when hull separation increases and increases with Froude number as discussed in previous section for hull without transom

stern, Wigley III. However, a ship without transom stern is not a good realistic representation for this type of applications. Hence, the investigation into the catamarans with transom stern is recommended.

NOMENCLATURE

B	Hull breadth *(m)*
C_B	Block coefficient (-)
C_F	Frictional resistance coefficient *(-)*
C_R	Residuary resistance coefficient *(-)*
C_T	Total resistance coefficient *(-)*
C_V	Viscous resistance coefficient *(-)*
C_W	Wave resistance coefficient *(-)*
Fn	Froude number *(-)*
g	Acceleration due to gravity *(m/s^2)*
L	Hull length *(m)*
Re	Reynolds' number *(-)*
S	Separation distance between the centerlines of demihulls *(m)*
T	Hull draught *(m)*
y^+	Dimensionless wall distance *(-)*
$(1+k)$	Form factor *(-)*
β	Viscous resistance interference factor *(-)*
ζ	Wave Elevation (*m*)
ρ	Density of water *(kg/m^3)*
τ	Wave resistance interference factor *(-)*
σ	Frictional resistance interference factor *(-)*
∇	Displacement volume *(m^3)*

REFERENCES

[1] Insel, M. and Molland, A.F. An investigation into resistance components of high-speed displacement catamarans, Transaction of the Royal Institute of Naval Architects, Vol. 134, 1992, pp. 1-20.

[2] Molland, A.F., Wellicome, J.F. and Couser, P.R. Resistance experiment on a systematic series of high speed displacement catamaran forms: Varian of length-displacement ratio and breadth-draught ratio, Ship Science Report 71, Southampton: University of Southampton, 1996.

[3] Utama, I.K.A.P. Investigation of the viscous resistance components of catamaran forms, PhD Thesis, 1999, University of Southampton, Southampton.

[4] Morarez, H., Vasconcellos, J. and Latorre, R. Wave resistance for high-speed catamarans, Ocean Engineering, Vol. 31(17), 2014, pp. 2253-2282.

[5] Pranzitelli, A., Nicola, C. and Miranda, S. Steady-state calculations of free surface flow around ship hulls and resistance predictions, paper presented in High Speed Marine Vehicles (IX HSMV), 2011, Naples, Italy.

[6] Wackers, J., Koren, B., Raven, H.C., van der Ploeg, A., Starke, A.R., Deng, G.B. et al. Free-surface viscous flow solution methods for ship hydrodynamics, Archives of Computational Methods in Engineering, Vol. 18(1), 2011, pp. 1-41.

[7] Larsson, L., Stern, F. and Visonneau, M. Gothenburg 2010, A workshop on numerical ship hydrodynamics. Gothenburg, Sweden, 2010.

[8] Aktar, S., Saha, G.K. and Alim, M.A. Drag analysis of different ship models using computational fluid dynamics tools. paper presented in the 6th International Conference on Marine Technology MARTEC 2010, Dhaka, Bangladesh.

[9] Zha, R., Ye, H., Shen, Z. and Wan, D. Numerical computations of resistance of high-speed catamaran in calm water, Journal of Hydrodynamics, Ser. B, Vol.26(6), 2014, pp. 930-938.

[10] Samuel, S.I.M. and Utama, I.K.A.P. An investigation into the resistance components of converting a traditional monohull fishing vessel into catamaran form, International Journal of Technology, Vol. 6(3), 2015, pp. 432-441.

[11] Froude, W. Experiments on the surface-friction experienced by a plane moving through water, Report of British Association for the Advancement of Science, 1872.
[12] Hughes, G. Friction and form resistance in turbulence flow and a proposed formulation for use in model and ship correlation, Transaction of the Royal Institute of Naval Architects, Vol. 96, 1954, pp. 314-376.
[13] Kasahara, M. and Masuda, S. Verification of simulation flow field around ships by using CFD Code, Paper presented at the Proceedings of the Third Osaka Colloquium Advanced CFD Applications to Ship Flow and Hull Form Design, 1998, Osaka, Japan.
[14] Larsson, L., Stern, F. and Bertram, V. Gothenburg 2000, A workshop on numerical ship hydrodynamics, Gothenburg, Sweden, 2002.
[15] Hino, T. CFD workshop Tokyo 2005, National Maritime Research Institute, Japan, 2005.
[16] ITTC. Report of the Resistance Committee, Proceedings of the 23rd International Towing Tank Conference, 2002, Venice, Italy.
[17] Srinakaew, S., Taunton, D.J. and Hudson, D.A. A study of resistance of high-speed catamarans and scale effects on form factor, paper presented in proceeding of the 19th Numerical Towing Tank Symposium (NUTTS'16), 2016, St Pierre d'Oleron, France.